

Functional TIM10 Chaperone Assembly Is Redox-regulated *in Vivo**

Received for publication, December 1, 2003, and in revised form, January 20, 2004
Published, JBC Papers in Press, February 18, 2004, DOI 10.1074/jbc.M313045200

Hui Lu‡, Scott Allen‡, Leanne Wardleworth‡, Peter Savory‡, and Kostas Tokatlidis‡§¶

From the ‡School of Biological Sciences, University of Manchester, Oxford Road, Manchester M13 9PT, United Kingdom, §Department of Chemistry, University of Crete, P. O. Box 1470, 714 09 Heraklion, Greece, and Institute of Molecular Biology and Biotechnology-Foundation for Research and Technology (IMBB-FORTH), P. O. Box 1527, 711 10 Heraklion, Greece

The TIM10 chaperone facilitates the insertion of hydrophobic proteins at the mitochondrial inner membrane. Here we report the novel molecular mechanism of TIM10 assembly. This process crucially depends on oxidative folding in mitochondria and involves: (i) import of the subunits in a Cys-reduced and unfolded state; (ii) folding to an assembly-competent structure maintained by intramolecular disulfide bonding of their four conserved cysteines; and (iii) assembly of the oxidized zinc-devoid subunits to the functional complex. We show that intramolecular disulfide bonding occurs *in vivo*, whereas intermolecular disulfides observed *in vitro* are abortive intermediates in the assembly pathway. This novel mechanism of compartment-specific redox-regulated assembly is crucial for the formation of a functional TIM10 chaperone.

Cysteine has unique biological functions by using its sulfhydryl (–SH) group in the active site of an enzyme, in chelating metals, or as the active site of disulfide reshuffling. For example, in the case of the molecular chaperone, Hsp33 activity is regulated by a redox switch with its inactive form reduced and zinc-coordinated and its active form turned on by oxidation and disulfide formation (1). The transcription factor OxyR is similarly activated through the formation of a disulfide bond and inactivated by enzymatic reduction with glutaredoxin (2). Disulfide bond formation in general is an essential step in the folding of many proteins, and it is catalyzed *in vivo* by the *dsb* system in the bacterial periplasm (3) and the functionally related *PDI/Ero1* (4) system in the ER of eukaryotic cells. Although a mitochondrial intermembrane space sulfhydryl oxidase, Erv1p, has been identified (5), there has been no report suggesting disulfide bond formation in mitochondria. Here we demonstrate that the mitochondrial intermembrane space can allow oxidative folding events, challenging the commonly accepted notion that this compartment is in complete redox equilibrium with the reducing cytosol. We show that substrates for this oxidation event are Tim9 and Tim10, the subunits of the TIM10 chaperone that mediates hydrophobic protein insertion at the inner mitochondrial membrane (6–9). This complex binds to the hydrophobic segments of the precursor (10) at an early import stage as the precursor emerges from the outer

membrane protein import channel (translocase of the outer membrane, TOM¹ complex). Subsequently, the precursor is carried across the intermembrane space and passed onto the TIM22 membrane-embedded complex that facilitates insertion (11–13) through a twin pore involving two voltage-dependent steps (14).

As all of the TIM subunits are imported themselves from the cytosol, correct assembly to their respective complex is essential for their function. Tim9 and Tim10 partner each other specifically to form the TIM10 complex, but the structural basis and the mechanism of this assembly process remain unclear. Although the “twin CX3C” motif common to all of the small Tim proteins is thought to be important for the structural integrity of the assembled complex (10, 15–17), Sirrenberg *et al.* (18) suggest that this motif binds zinc, whereas Curran *et al.* (10) contradict this by suggesting that in the purified complex the Cys residues are rather involved in disulfide bridges. However, these reports have not addressed which are the productive Tim9 and Tim10 species that can form a complex, the mechanism of import, folding, and subsequent complexation for the individual subunits and how assembly is regulated by redox state, these all being important questions that remain unresolved.

The TIM10 complex is a recently discovered chaperone (19), and in contrast to most well characterized chaperone systems, it interacts with membrane proteins and does not require ATP hydrolysis for its function. The fact that it is made up of two different subunits raises additional important questions regarding its assembly and function. We report the novel assembly mechanism of the TIM10 chaperone particle, its mode of regulation by redox state, and how this underpins the different stages of import and assembly. All four cysteines of the “twin CX3C” must be kept in a reduced state for import to occur. After passage across the outer membrane, the “twin CX3C” motifs are intramolecularly disulfide-bonded by a novel oxidative folding mechanism. The complex is made only from the oxidized subunits, whereas intermolecular disulfides result in abortive misfolded species. Zinc does not play a role in complex formation. Organelle-specific redox regulation is thus essential for the assembly of the TIM10 complex into a biologically functional state in its physiological environment.

EXPERIMENTAL PROCEDURES

Circular Dichroism Spectroscopy—CD spectra were acquired using a JASCO J810 spectropolarimeter in 5 mM Tris (pH 7.6) at 25 °C using a 1-mm cuvette and protein samples of 0.05 and 0.07 mg/ml for Tim9 and

* This work was supported by the Wellcome Trust, the Medical Research Council (MRC), Biotechnology and Biological Sciences Research Council, and the Leverhulme Trust (to K. T.) and an MRC co-operative group grant (to K. T.). The costs of publication of this article were defrayed in part by the payment of page charges. This article must therefore be hereby marked “advertisement” in accordance with 18 U.S.C. Section 1734 solely to indicate this fact.

¶ A Lister Institute Research Fellow. To whom correspondence should be addressed. Tel.: 30-2819-391136; Fax: 30-2810-391101; E-mail: tokatlid@imbb.forth.gr.

¹ The abbreviations used are: TOM, translocase of the outer membrane; TIM, translocase of the inner membrane; DTT, dithiothreitol; Tricine, *N*-[2-hydroxy-1,1-bis(hydroxymethyl)ethyl]glycine; WT, wild type; NEM, *N*-ethylmaleimide; DTNB, 5,5'-dithiobis(nitrobenzoic acid); AMS, 4-acetamido-4'-maleimidylstilbene-2,2'-disulfonic acid; TCEP, Tris[2-carboxyethyl]phosphine.

Tim10, respectively. The spectra of the DTT- and/or GdnHCl-denatured states were recorded after overnight incubation at 4 °C or ~4 h at room temperature. Each spectrum represents an average of four scans from 260 to 190 nm at 0.2-nm intervals, and the base line is established by subtracting spectrum of the buffer. The signals are normalized by the total number of residues (87 for Tim9 and 93 for Tim10).

AMS Alkylation Assay—The purified Tim9 and Tim10 (5–10 μg each) in 50 mM Tris (pH 7.4), 150 mM NaCl, either left untreated or reduced with 1 mM TCEP (a reducing agent) at 4 °C overnight, were incubated with 1 mM of thiol-specific alkylating reagent AMS (Molecular Probes) at 4 °C overnight in dark. SDS-PAGE gel sample buffer with or without DTT was then added, and the samples were analyzed by 16% Tricine SDS-PAGE followed by Coomassie Blue staining. AMS, a 500-Da molecule, reacts with free thiols of cysteine residues in a protein at 1:1 ratio resulting in a visible mobility shift on SDS-PAGE.

Isothermal Titration Calorimetry—The binding of Tim9 to Tim10 was tested in 20 mM sodium phosphate (pH 7.6) at 30 °C with a VP-ITC microcalorimeter. Tim9 or Tim10 was in the 1.4-ml cuvette at 10 μM , and 35 injections of 5 μl of 150 μM Tim10 or Tim9 were made. Protein concentration was determined by both the Bradford assay and amino acid analysis. The data were analyzed and best fitted to a one-site model.

Determination of Redox State of Tim10 in Vivo—Yeast cells (20 optical density units) were harvested and suspended in 200 μl of 10% trichloroacetic acid on ice for 1 h, and proteins were collected by centrifugation. Protein pellet was washed with 200 μl of ice-cold acetone. Proteins then were solubilized in 100 μl of 2 \times non-reducing sample buffer containing 4% SDS, 0.5 M Tris (pH 8) and heated up at 95 °C for 5 min. 4% SDS keeps proteins in a denatured state. The solubilized proteins were divided into three samples. The first one was left untreated and used as a negative control. The second one was incubated with 30 mM AMS at room temperature for 1 h. The third sample was a positive control to which 10 mM TCEP was added at room temperature for 1 h to reduce disulfides followed by the addition of 30 mM AMS and incubation at room temperature for 1 h. For the analysis of protein redox states in yeast cells pretreated with DTT, the cells (20 optical density units) first were suspended in 100 μl of 150 mM NaCl, 50 mM Tris buffer (pH 7.4) containing 0 or 200 mM DTT at 37 °C for 30 min and then TCA and AMS treatments were then carried out exactly as above. For the analysis of protein redox states in mitochondria, four samples of 0.25 mg of purified mitochondria were used. For the negative control and experiment, mitochondria were solubilized in 20 μl of non-reducing gel sample buffer containing 4% SDS, 0.5 M Tris (pH 8) in the presence of 0 and 10 mM AMS at 37 °C for 1 h covered with foil. For the two positive controls, mitochondria first were solubilized in 20 μl of non-reducing gel sample buffer plus 10 mM TCEP or 10 mM DTT at 37 °C for 1 h to reduce proteins and then 15 mM AMS was added to each sample and incubated at 37 °C again for 1 h covered with foil. Finally, all of the samples were analyzed on 16% Tris-Tricine SDS-PAGE followed by Western blotting with antibodies against Tim10.

Protein Import Experiments—The purified oxidized and reduced Tim10 was imported into purified tim9-ts (temperature-sensitive) mitochondria as described previously (8). 20 μl of 0.1 mg/ml (10 μM) Tim10 in the buffer A (50 mM Tris (pH 7.4), 150 mM NaCl) in the absence (oxidized) or presence of 10 mM DTT and 0–50 μM ZnCl₂ (reduced \pm Zn²⁺) on ice for 1 h were prepared before import experiments. 200 μg (0.4 ml of 0.5 mg/ml) of purified tim9-ts mitochondria were incubated with 2 μg of purified Tim10 at different states for 15 min at 30 °C in import buffer in the presence of 5 mM NADH and 5 mM ATP (20). Mitochondria were harvested by centrifugation and incubated with 200 μl of breaking buffer (20 mM HEPES (pH 7.4), 0.6 M sorbitol) containing 0.1 mg/ml proteinase K for 10 min on ice and then inhibited with 1 mM phenylmethylsulfonyl fluoride. Mitochondria were then re-isolated by centrifugation, solubilized in 50 μl of sample buffer, and loaded on a 16% Tris-Tricine SDS-PAGE.

For import of radioactive precursors, WT and Cys mutants ³⁵S-labeled were prepared using rabbit reticulocyte *in vitro* translation. The Cys mutants of Tim10 were subcloned into pSP64 as BamHI/EcoRI fragments from the corresponding pGEX 4T1 plasmids (21). NEM-alkylated [³⁵S]Tim10 was made by incubation with 2 mM NEM on ice for 1 h before import. 20 μl of radioactive precursor was added to 200 μg (0.4 ml of 0.5 mg/ml) of wild type mitochondria. Each sample was then halved and analyzed by 16% Tris-Tricine SDS-PAGE or 6–16% Blue-Native-PAGE (8). The redox state of the WT [³⁵S]Tim10 and the NEM-alkylated precursor were analyzed by incubating with 5 mM AMS on ice for 1 h followed by 16% Tris-Tricine SDS-PAGE. Radioactive proteins were visualized by autoradiography using a Fuji Bas station, version 1.3.

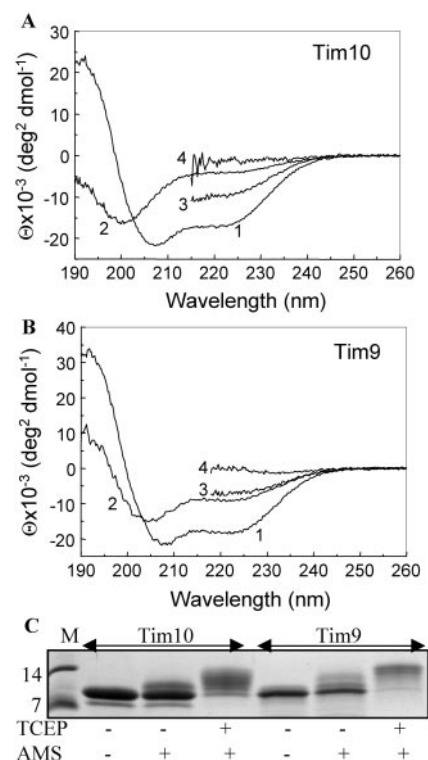


FIG. 1. Oxidized and reduced states of Tim9 and Tim10. A–B, far-UV CD spectra of Tim10 (panel A) and Tim9 (panel B) in 5 mM Tris buffer (pH 7.6) (trace 1) containing 1 mM DTT (trace 2) and in 6 M GdnHCl without (trace 3) or with (trace 4) 1 mM DTT. Each spectrum is an average of four scans. Deconvolution of the spectra indicated: (i) oxidized Tim10: 65% α -helix, 35% coil; (ii) reduced Tim10 (+TCEP): 8% α -helix, 33% β -sheet, 59% coil; (iii) Tim9: 53% α -helix, 8% β -sheet, 38% coil; and (iv) reduced Tim9 (+TCEP): 12% α -helix, 39% β -sheet, 49% coil. TCEP was used instead of DTT in these experiments because deconvolution was more conveniently done and more reliable. Note that for Tim10, the DTT-reduced state (trace 2) is more unfolded than the 6 M GdnHCl-denatured state (trace 3) with the protein being fully unfolded when both DTT and GdnHCl were present (trace 4). For Tim9, the spectrum of DTT-reduced Tim9 is similar to that of the GdnHCl-denatured Tim9, suggesting a weaker unfolding of Tim9 by DTT alone compared with Tim10. C, AMS alkylation of the oxidized and 1 mM TCEP reduced proteins separated by 16% Tris-Tricine SDS-PAGE followed by Coomassie Blue staining.

RESULTS

Folding of Tim9 and Tim10 Depends on Their Redox State—Tim9 and Tim10 are part of the “tiny Tims” family of proteins that all share a strictly conserved “twin CX3C” motif suggested to be important for their function (10, 18, 21). We examined the role of these four Cys in maintaining the structure of Tim9 and Tim10. To this end, we used structural techniques like CD and NMR as well as chemical modification with AMS and DTNB. As shown by far-UV CD spectra (Fig. 1, A and B) in the absence of a reducing agent, both proteins are folded and are mainly α -helical, in agreement with secondary structure predictions. When the thiol-reducing agent, DTT, was added to the folded native proteins, they both became unfolded in a DTT concentration-dependent manner to a state similar or even less folded than the guanidine-denatured state (Fig. 1, A and B, compare traces 1 and 2). Their α -helical content decreased dramatically with a concomitant increase in coil content (reaching 50–60%) and a slight increase in β -sheet content (see legend to Fig. 1). In both cases, disulfide bonds are crucial in stabilizing the secondary structure of the native state, which can be unfolded by a thiol-reducing agent alone. These results were expanded by a more detailed structural study at atomic resolution using NMR and SAXS (33).

As the disulfide bonds play a crucial role, the redox status of the thiol groups was measured directly by thiol trapping with AMS (22) and DTNB (23). As shown in Fig. 1C, AMS reacted with the protein only when this was pre-reduced by TCEP, suggesting that all of the cysteines are disulfide-bonded in their native states. The weak new bands of Tim10 and Tim9 in the sample without TCEP (*lanes 2 and 5*) presumably arise from partially oxidized species during protein purification. These are not observed in the endogenous proteins and in the complex (Fig. 3). DTNB assays further confirmed this result and suggested that there are no free thiols in the oxidized state and four free thiols in the reduced state. Therefore, under native conditions, both Tim10 and Tim9 are oxidized and partially folded with mainly α -helix, whereas in the presence of a reducing agent, they become unfolded. In the accompanying paper (33), we show that zinc binds only to the reduced Tim9 and reduced Tim10 and it does not influence the secondary structure and stabilizes the reduced state against proteolytic degradation.

The TIM10 complex can assemble only from the oxidized, zinc-devoid subunits—The existence of the two proteins in two structurally distinct redox states suggested that the assembly process is regulated by the cellular redox conditions and raised the question which are the productive structural intermediates in the assembly pathway. Fig. 2A shows that the TIM10 complex, eluted at ~ 10 ml in a Superdex 75 gel filtration column, formed only when Tim9 and Tim10 were oxidized (*solid line*). This coincides with the elution profile of the authentic complex purified from mitochondria (19). The reduced apoproteins (treated with EDTA, *dashed line*) eluted at ~ 12 ml. This is the same elution volume as the individual unassembled proteins, indicating no complex formation between the reduced forms of the proteins. Zinc binding (*dotted line*) does not promote any complex formation between the reduced proteins. Consistent results were obtained by ITC measurements (Fig. 2B), and the binding constant for the oxidized subunits was $3 \pm 1 \times 10^7 \text{ M}^{-1}$. Further ITC measurements show that although zinc can bind to both reduced Tim9 and Tim10 at 1:1 ratio, it cannot bind to the pre-formed TIM10 complex, excluding the possibility of an equilibrium between the oxidized and reduced states. Taken together, these data show that the TIM10 complex can only form from oxidized subunits.

DTT reduction and unfolding is a very sensitive and appropriate assay for this system and was thus applied as shown in Fig. 2C. The disulfide bonds of Tim9 and Tim10 in the complex are resistant to DTT reduction and unfolding, showing that they are extremely stable and possibly buried upon assembly, in sharp contrast to the unassembled Tim9 or Tim10 where they are readily reduced. This structural rearrangement upon assembly may also explain our previous observation that the individual subunits become more resistant against proteolysis when assembled into the TIM10 complex (19). AMS and DTNB assays confirmed that all of the Cys residues are involved in disulfide bonds within the complex.

In Vivo Redox State of TIM10—The above detailed analysis and previous experiments with purified complex from mitochondria (10) strongly suggested that *in vivo* the Cys residues of the TIM10 complex are oxidized. To unambiguously determine the redox state of the Cys residues *in vivo*, we examined (i) intact yeast cells and (ii) import-competent intact mitochondria. Treatment of yeast cells with trichloroacetic acid rapidly lowers intracellular pH, thereby blocking any possible thiol-disulfide exchange and “freezing” existing disulfides. Subsequently, the proteins are solubilized in a non-reducing sample buffer containing 4% SDS and 0.5 M Tris (pH 8), which keeps them denatured, and free cysteinyl residues are determined by

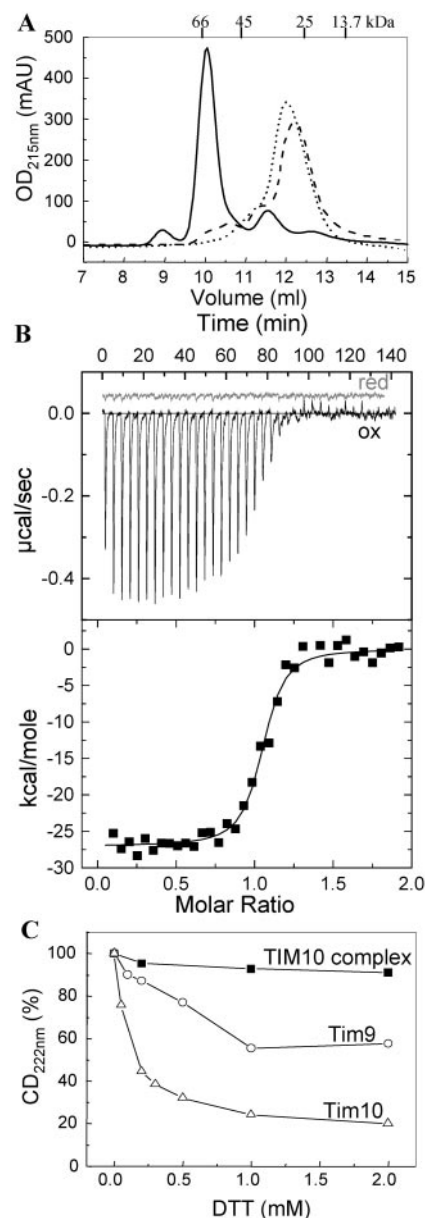


FIG. 2. **The TIM10 complex formation.** A, Superdex 75 size exclusion profiles of the mixtures of purified Tim9 and Tim10 at a ratio of 1:1 in 50 mM Tris, 150 mM NaCl (pH 7.4) (19). Both proteins were in the oxidized forms (*solid line*), 1 mM DTT-reduced form in the presence of 1 mM EDTA (*dashed line*), and 1 mM DTT-reduced form in the presence of 50 μM ZnCl_2 (*dotted line*). Molecular mass markers (in kDa) are indicated at the top of the graph. B, ITC measurements of the binding reaction of the oxidized proteins (*black line, ox*) and the reduced proteins (*gray line, red*) in 20 mM sodium phosphate buffer (pH 7.4) at 30 °C. C, DTT-dependent unfolding of Tim10, Tim9, and the TIM10 complex.

AMS analysis (24). Fig. 3A shows these results *in vivo* for Tim10 that AMS treatment in the absence of TCEP does not affect the protein (compare *lanes 1 and 2*). In contrast, AMS treatment following preincubation with TCEP results in a quantitative shift of ~ 2 kDa with AMS addition (*lane 3*), consistent with all four Cys residues having reacted with AMS (500 Da). This finding suggests that all four Cys residues are disulfide-bonded *in vivo*. To exclude the possibility that oxidation of Tim10 by oxygen occurs during or after solubilization in this experiment, we pretreated the cells with 200 mM DTT before the analysis. *Lane 7* shows that Tim10 in DTT-reduced cells is shifted by 2 kDa with AMS addition (compared with *lane 6* in the absence of AMS and to untreated cells in *lanes 4*

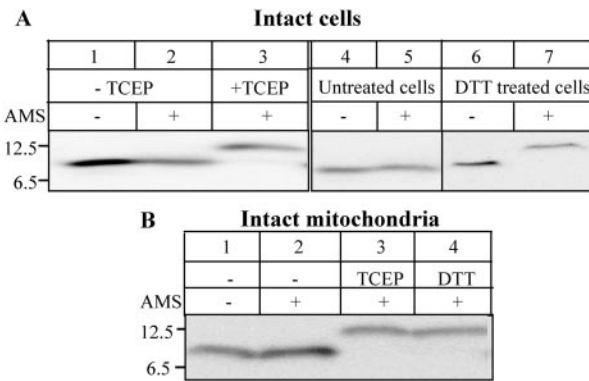


FIG. 3. *In vivo* redox state of Tim10. *A*, redox state analysis of Tim10 in intact yeast cells, AMS assay of Tim10 following trichloroacetic acid treatment of the cells and SDS solubilization/denaturation (lanes 1–5). The proteins were without (lanes 1, 2, 4, and 5) and with 10 mM TCEP (lane 3) treatment before AMS assay. AMS assay of the mock-treated cells (lanes 4 and 5) and cells pretreated with 200 mM DTT (lanes 6 and 7) is shown. *B*, redox state analysis of Tim10 in mitochondria. Mitochondria were solubilized and assayed in the buffer containing 0 (lane 1) and 10 mM AMS (lane 2). For the positive controls, mitochondria were solubilized in the buffer containing 10 mM TCEP (lane 3) or 10 mM DTT (lane 4) before 15 mM AMS was added.

and 5). Residual DTT cannot be present because (i) the samples were precipitated by trichloroacetic acid and washed in acetone and (ii) we observed a quantitative and complete shift of all of the protein molecules rather than a partial shift. This finding unequivocally shows that Tim10 cannot be oxidized during solubilization from its reduced state under these conditions and reinforces the notion that these results are a true reflection of the *in vivo* situation. Finally, the redox state of the protein in intact import-competent mitochondria was performed and gave identical results (Fig. 3*B*). In these experiments, the isolated mitochondria were directly solubilized in the buffer containing AMS without any prior trichloroacetic acid precipitation. The same results were observed for Tim9 (data not shown). Therefore, both Tim9 and Tim10 are oxidized *in vivo*.

Intermolecular Disulfides Are Abortive Intermediates in the TIM10 Assembly Pathway—A usual problem in the folding of proteins dependent on disulfide bonds is the formation of the correct ones, which is a process facilitated *in vivo* by protein-disulfide isomerases (3, 4). In this vein, we examined whether, during folding and *in vitro* assembly of the Tim9 and Tim10 subunits, intermolecular disulfide bonds could form as well and how they influence proper complex formation (Fig. 4). The individual oxidized proteins were mixed together and run on gel filtration, and the different fractions were analyzed on SDS-PAGE \pm DTT to reveal possible intermolecular disulfide-bonded molecules. Fraction 10 that corresponded to the 70-kDa TIM10 complex was essentially devoid of disulfide-bonded dimeric Tim9 or Tim10. However, fractions 11 and 12 that correspond to mis-assembled species only observed *in vitro* contained a very high proportion of covalent homodimers that are intermolecularly disulfide-bonded Tim9 and/or Tim10. These misfolded species represent abortive intermediates in the TIM10 assembly pathway. In contrast, non-covalent homodimers can dissociate to give monomers that could subsequently associate to form the proper hetero-hexameric complex of three Tim10 and three Tim9 molecules. Consistent with this model for assembly, we find that complex formation is more efficient when the fractions of Tim9 and Tim10 that are mixed together are enriched in monomeric rather than dimeric species (data not shown).

Mechanism of TIM10 Assembly in Vivo—What is the sequence of events for assembly *in vivo*, and how do our *in vitro* results reflect the situation in the cell? To address these ques-

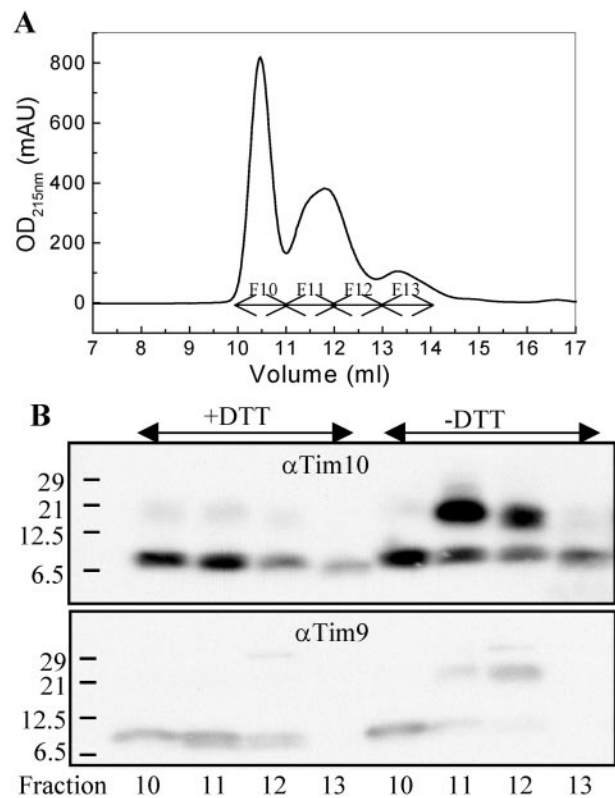
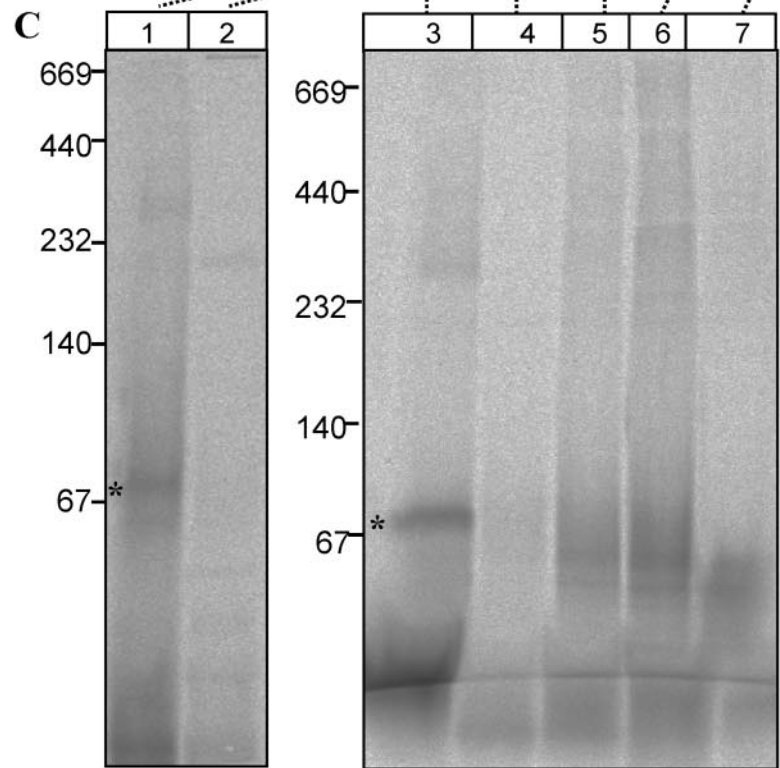
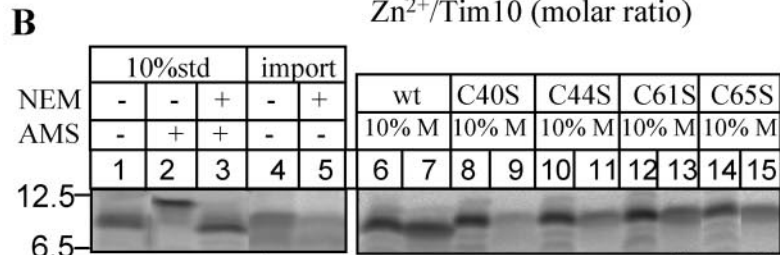
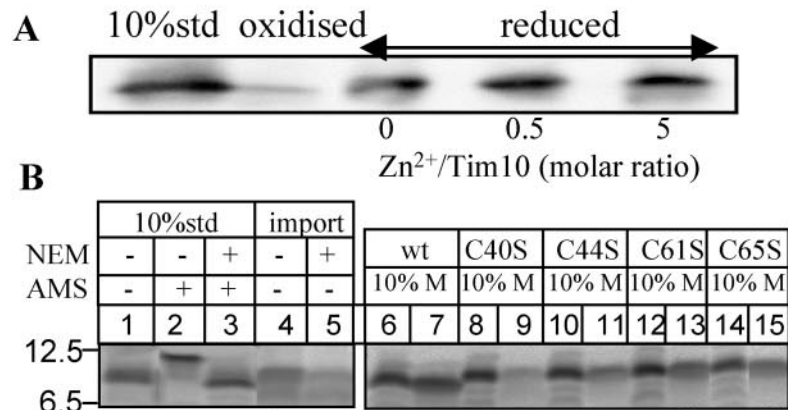


FIG. 4. *Intermolecular disulfide-bonded molecules are abortive assembly intermediates*. *A*, gel filtration of a mixture of natively oxidized and intermolecularly bonded misfolded complex species. A Superdex 75 size-exclusion profile of oxidized Tim9 and Tim10 at a ratio of 1:1 is shown. *B*, Western blotting analysis for panel *A*. Fractions 10–13 were analyzed by SDS-PAGE using a sample buffer with or without DTT. The gels were followed by immunoblotting using rabbit anti-Tim9 or anti-Tim10 polyclonal antibodies.

tions, we examined the import of purified Tim10 at different states using isolated temperature-sensitive tim9 mitochondria that lacked both Tim9 and Tim10. Western blotting of the imported protein (Fig. 5*A*) shows that the oxidized form cannot be imported despite being only partially folded, in contrast to the reduced protein that is efficiently imported. There was no obvious effect on the level of import by the presence of up to five times the concentration of ZnCl₂. These results are consistent with the folding state of the protein. It appears that import requires that even these small proteins (10 kDa) must be fully reduced, hence unfolded. In contrast, the more but still partially folded oxidized form cannot be imported. These data are in agreement with the general notion that unfolding of a polypeptide targeted to the matrix facilitates passage across the TOM channel. Folding by creation of disulfide bonds imposes steric constraints of the folded domains to pass through the outer membrane import pore (25, 26). These studies only dealt with precursors that have to pass through both the outer and inner membrane channels and significantly interact with the translocation motor mitochondrial Hsp70 that actively unfolds the protein (26). Our data extend these important previous findings. Even in the case of small proteins (10 kDa) that are intrinsically only partially folded and that only have to be translocated through a single import channel (the TOM complex), independent of the inner membrane potential, import can only occur in the fully reduced unfolded state.

These results were confirmed in two ways in import experiments using ³⁵S-labeled Tim10 either NEM-alkylated or mutated in each Cys. NEM-alkylated protein could still be imported (Fig. 5*B*, lanes 4 and 5). As a control, AMS assay is also



D

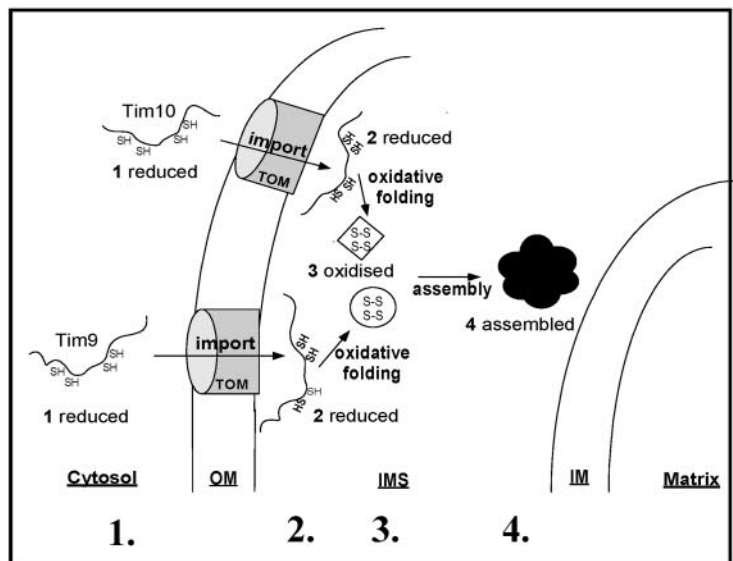


FIG. 5. Effect of Cys oxidation in Tim10 import and retention. *A*, import of purified Tim10 into purified tim9-ts mitochondria. The oxidized Tim10 and reduced Tim10 (20 μ l at 10 μ M) in the presence of 0–5 molar ratio of ZnCl₂:protein was imported into purified tim9-ts mitochondria, re-isolated, and analyzed by SDS-PAGE and Western blotting. *B*, import of [³⁵S]Tim10 (WT or Cys mutants) into purified mitochondria. All of the samples were analyzed by 16% Tris-Tricine SDS-PAGE and autoradiography. *Lanes 1–5*, effect of NEM alkylation on import of WT Tim10; *lanes 6–15*, effect of Cys mutagenesis on the import of Tim10. *C*, Blue-Native-PAGE, import of radioactive [³⁵S]Tim10 precursor and Cys mutants as shown in *B*. Corresponding SDS-PAGE samples from *B* are indicated by the dotted lines. The molecular masses of markers provided are in kDa. *D*, model for the mechanism of TIM10 assembly *in vivo* mediated by redox state. *Stage 1*, cytosolic forms in a reduced and unfolded state; *stage 2*, imported forms in a reduced state that is not competent for assembly; *stage 3*, oxidized and partially folded state that is assembly-competent; *stage 4*, fully assembled functional complex. Transition from stage 2 to stage 3 *in vivo* depends on intramolecular disulfide bonds created by as yet unidentified protein(s). *In vitro*, stage 3 may also contain intermolecular disulfides that are dead-end products in the assembly pathway. Stage 4 is made exclusively from intramolecularly disulfide-bonded Tim9 and Tim10.

indicated (Fig. 5B, lanes 1–3). Strikingly, NEM-alkylation had a detrimental effect on complex formation as monitored by Blue-Native-PAGE (compare corresponding lanes 1 and 2 in Fig. 5C; the WT 70-kDa complex is indicated by an *asterisk*). These data confirm our results and show that blocking disulfide bonding by irreversible alkylation completely abolishes complex formation *in organello*. In the same vein, a similar effect was observed when any of the four Cys residues was exchanged to a Ser. All of the mutants could still import into mitochondria (Fig. 5B, lanes 6–15) but were not able to form the 70-kDa complex (Fig. 5C, lanes 4–7) in contrast to the WT (indicated by an *asterisk*, lane 3). The results of the Cys mutations here are in agreement with those obtained for a Cys to Trp mutation of the fourth Cys in the homologous Tim8 protein (16, 17).

Taken together, our data would support the following redox-regulated multi-step mechanism of biogenesis and assembly of the TIM10 complex (Fig. 5D). (i) The individual subunits Tim9 and Tim10 are kept in a reduced and unfolded state in the cytosol (stage 1). (ii) The reduced and unfolded proteins are imported through the outer membrane pore (27) into the intermembrane space in a reduced assembly-incompetent state (stage 2). Zinc may bind at this stage to protect these species from proteolysis. However, it must be readily released for oxidative folding to occur. (iii) Oxidative folding of the two subunits in the intermembrane space is then facilitated by as yet unknown protein(s). Intramolecular disulfides (21) maintain this state to an oxidized assembly-competent conformation (stage 3). (iv) The two oxidized subunits strongly bind to each other to give the fully functional TIM10 particle (stage 4). This novel mode of assembly for a chaperone particle relies on the redox state in a compartment-specific manner. The reduced state in the cytosol is vital for import, whereas rapid oxidative folding after import in mitochondria is crucial for assembly.

DISCUSSION

The above results clearly showed that the two proteins must be imported in a reduced state and then become oxidized in the intermembrane space. This was somewhat surprising as (i) it is generally accepted that the mitochondrial intermembrane space is in redox equilibrium with the reducing cytosol and (ii) no protein oxidase system has been described for the intermembrane space. Neither Tim9 nor Tim10 could oxidize each other (data not shown), suggesting that they must be independently oxidized before they interact. Is oxidation of Tim9 and Tim10 a spontaneous process? This is rather unlikely as (i) no misassembled intermolecular disulfide species are observed *in vivo*, (ii) the oxidation process is concomitant with a structural change, and (iii) oxidation *in organello* occurs considerably faster than *in vitro*. Complete oxidation of Tim9 or Tim10 occurred within 15 min of import into mitochondria compared with no oxidation at all *in vitro*. These observations strongly argue in favor of a protein-mediated oxidation process for Tim9 and Tim10. As the intermembrane space is related to the bacterial periplasm, one might expect that a functionally related mitochondrial homologue to dsbA (or PDI) might exist to ensure disulfide bonding of at least a subset of proteins. Indeed, a homologue of PDI has been reported to be associated with mitochondria (28) but its submitochondrial localization and exact function remain unknown. An obvious candidate for the oxidation equivalent needed in this process would be the electron transport chain of the inner membrane. In bacteria, the electron flow during oxidative folding in the periplasm involves the electron transport chain with O₂ as the terminal acceptor (29). We are currently investigating these questions for the oxidative folding pathway in mitochondria.

The fact that folding crucially depends on the correct in-

tramolecular disulfides provides a molecular explanation for the assumed important role of the “twin CX3C” motif in the assembly of the small TIM complexes because it maintains the individual subunits in the correct conformation to allow interaction. We have recently mapped the native disulfides of Tim10 and found that the four cysteines of the distal CX3C motifs are intramolecularly juxtaposed via an inner (Cys⁴⁴-Cys⁶¹) and an outer (Cys⁴⁰-Cys⁶⁵) disulfide (21). It remains an open possibility that other segments, unrelated to the “twin CX3C” motif, might be involved as the direct contact sites in the complex. These would only be able to bind although in the topology ensured by the intramolecular disulfides.

Previously, it was suggested based mainly on *in vitro* AMS labeling that the fully assembled TIM10 complex does not bind zinc and that the cysteines may be involved in disulfide bridges (10). Contradicting this report, Lutz *et al.* (30) recently published that the homologous Tim13 protein rather binds zinc and its cysteines are coordinated by the metal. However, no direct data on the capacity of the zinc-bound form to assemble to a complex were provided. Here we have used a combination of AMS labeling, DTNB assays, ITC, and CD to provide conclusive data that the cysteines are involved in intramolecular disulfides *in vitro*. Importantly, we show that this is the case in intact cells *in vivo* and also in import-competent intact mitochondria. Furthermore, we also show how we get to the fully assembled complex (Fig. 5D, stage 4). The complex can only be made by an interaction of oxidized subunits. The reduced subunits are completely assembly-incompetent, and the addition of zinc does not allow complexation. Furthermore, once the complex is made, the intramolecular disulfides become resistant to reduction, rendering the assembly process essentially irreversible. These results leave little doubt that TIM10 assembly is zinc-independent, a question previously unresolved. It remains open that zinc binding may occur to protect the protease-sensitive reduced states (stage 1 or 2 in the model of Fig. 5D) and/or as a transient intermediate leading up to the assembly-competent oxidized state. This would support a physiological role for zinc binding to the unassembled proteins. A recent publication reports that in human cells the interaction of DDP/Tim8 (a homologue of Tim9 and Tim10) with the signal-transducing adaptor molecule STAM1 in the cytosol is stimulated by zinc (31). Although the low average concentration of free zinc in the cytosol (nanomolar to picomolar range) (32) together with the relatively weak affinity would suggest that the fraction of zinc-bound Tim9 or Tim10 *in vivo* may be very low, this could be reversed by a locally high zinc concentration and/or some (as yet unidentified) dedicated zinc-dependent chaperone.

Alkylated Tim10 or Tim10 Cys mutants were clearly unable to form a complex after import into isolated mitochondria, confirming the validity of our data *in organello*. Interestingly, although both alkylated Tim10 and the Cys mutants could be imported, the level of import was less than the WT. These constitute direct data in favor of the idea that proper folding and assembly of the protein in the intermembrane space provides the driving force for rendering import unidirectional (30).

Based on these data, we postulate the presence of a novel disulfide catalytic machinery in mitochondria that facilitates the creation of disulfides in the small Tims and possibly other intermembrane space proteins as well. Identification of the components of this machinery is the next challenge and will enhance our understanding of the mechanism of this novel mitochondria-specific oxidative folding pathway in the cell.

Acknowledgments—We thank Neil Bulleid, Paula Booth, Tassos Economou, Dave Thornton, and our laboratory for discussions and comments on the paper, Paul Scott for help with CD data deconvolution, and Sarah Vial for help at the initial stages of this work.

REFERENCES

1. Jakob, U., Muse, W., Eser, M., and Bardwell, J. C. (1999) *Cell* **96**, 341–352
2. Choi, H., Kim, S., Mukhopadhyay, P., Cho, S., Woo, J., Storz, G., and Ryu, S. (2001) *Cell* **105**, 103–113
3. Ritz, D., and Beckwith, J. (2001) *Annu. Rev. Microbiol.* **55**, 21–48
4. Frand, A. R., Cuzzo, J. W., and Kaiser, C. A. (2000) *Trends Cell Biol.* **10**, 203–210
5. Lee, J., Hofhaus, G., and Lisowsky, T. (2000) *FEBS Lett.* **477**, 62–66
6. Adam, A., Endres, M., Sirrenberg, C., Lottspeich, F., Neupert, W., and Brunner, M. (1999) *EMBO J.* **18**, 313–319
7. Koehler, C. M., Merchant, S., Oppliger, W., Schmid, K., Jarosch, E., Dolfini, L., Junne, T., Schatz, G., and Tokatlidis, K. (1998) *EMBO J.* **17**, 6477–6486
8. Luciano, P., Vial, S., Vergnolle, M., Dyall, S., Robinson, D., and Tokatlidis, K. (2001) *EMBO J.* **20**, 4099–4106
9. Pfanner, N., and Geissler, A. (2001) *Nat Rev. Mol. Cell Biol.* **2**, 339–349
10. Curran, S. P., Leuenberger, D., Oppliger, W., and Koehler, C. M. (2002) *EMBO J.* **21**, 942–953
11. Bauer, M. F., Hofmann, S., Neupert, W., and Brunner, M. (2000) *Trends Cell Biol.* **10**, 25–31
12. Chacinska, A., Pfanner, N., and Meisinger, C. (2002) *Trends Cell Biol.* **12**, 299–303
13. Tokatlidis, K., and Schatz, G. (1999) *J. Biol. Chem.* **274**, 35285–35288
14. Rehling, P., Model, K., Brandner, K., Kovermann, P., Sickmann, A., Meyer, H. E., Kuhlbrandt, W., Wagner, R., Truscott, K. N., and Pfanner, N. (2003) *Science* **299**, 1747–1751
15. Curran, S. P., Leuenberger, D., Schmidt, E., and Koehler, C. M. (2002) *J. Cell Biol.* **158**, 1017–1027
16. Hofmann, S., Rothbauer, U., Muhlenbein, N., Neupert, W., Gerbitz, K. D., Brunner, M., and Bauer, M. F. (2002) *J. Biol. Chem.* **277**, 3287–3293
17. Roesch, K., Curran, S. P., Tranebjaerg, L., and Koehler, C. M. (2002) *Hum. Mol. Genet.* **11**, 477–486
18. Sirrenberg, C., Endres, M., Folsch, H., Stuart, R. A., Neupert, W., and Brunner, M. (1998) *Nature* **391**, 912–915
19. Vial, S., Lu, H., Allen, S., Savory, P., Thornton, D., Sheehan, J., and Tokatlidis, K. (2002) *J. Biol. Chem.* **277**, 36100–36108
20. Tokatlidis, K. (2000) *Methods Enzymol.* **327**, 305–317
21. Allen, S., Lu, H., Thornton, D., and Tokatlidis, K. (2003) *J. Biol. Chem.* **278**, 38505–38513
22. Joly, J. C., and Swartz, J. R. (1997) *Biochemistry* **36**, 10067–10072
23. Ellman, G. L. (1959) *Arch. Biochem. Biophys.* **82**, 72
24. Frand, A. R., and Kaiser, C. A. (1999) *Mol. Cell* **4**, 469–477
25. Schwartz, M. P., Huang, S., and Matouschek, A. (1999) *J. Biol. Chem.* **274**, 12759–12764
26. Vestweber, D., and Schatz, G. (1988) *J. Cell Biol.* **107**, 2037–2043
27. Kurz, M., Martin, H., Rassow, J., Pfanner, N., and Ryan, M. T. (1999) *Mol. Biol. Cell* **10**, 2461–2474
28. Rigobello, M. P., Donella-Deana, A., Cesaro, L., and Bindoli, A. (2001) *Biochem. J.* **356**, 567–570
29. Bader, M., Muse, W., Ballou, D. P., Gassner, C., and Bardwell, J. C. (1999) *Cell* **98**, 217–227
30. Lutz, T., Neupert, W., and Herrmann, J. M. (2003) *EMBO J.* **22**, 4400–4408
31. Blackstone, C., Roberts, R. G., Seeburg, D. P., and Sheng, M. (2003) *Biochem. Biophys. Res. Commun.* **305**, 345–352
32. Fausto da Silva, J. J. R., and Williams, R. J. P. (2001) *The Biological Chemistry of the Elements: The Inorganic Chemistry of Life*. Oxford University Press, Oxford
33. Lu, H., Golovanov, A. P., Alcock, F., Grossmann, J. G., Allen, S., Lian, L.-Y., and Tokatlidis, K. (2004) *J. Biol. Chem.* **279**, 18959–18966